ALFRED-WEGENER-INSTITUT
HELMHOLTZ-ZENTRUM FÜR POLAR- UND MEERESFORSCHUNG

User Guide

July 2016

AWI CryoSat-2 Sea Ice Thickness Data Product (v1.2)

HELMHOLTZ ASSOCIATION

Authors

Stefan Hendricks **Alfred Wegener Institute**
Helmholtz Centre for
Polar and Marine Research
Bremerhaven

Robert Ricker **Alfred Wegener Institute**
Helmholtz Centre for
Polar and Marine Research
Bremerhaven

Veit Helm **Alfred Wegener Institute**
Helmholtz Centre for
Polar and Marine Research
Bremerhaven

This work was funded by the
German Ministry of Economics and Technology
(Grant 50EE1008)

Document Version

Rev 1.0	24. June 2013	Initial Version
Rev 1.1	14. August 2015	Added Section Changelog (Change of algorithm version) Added Section Known Issues Updated algorithm description (processor v1.1) Updated list of output parameters
Rev 1.2	09. June 2016	Updated Changelog (processor v1.2) Added status/affected to known issues Updated algorithm description Added section for impact of algorithm changes

Important Note

This service does not intent to be an operational data service. Updates on monthly ice thickness fields will happen irregularly and revisions of the entire data time series might occur at any time. We stress the fact that the interpretation of CryoSat-2 radar signals over sea ice and the uncertainties of freeboard retrieval and conversion into sea ice thickness are still an active field of research. This product shall therefore be a tool for the scientific community to enable further development of sea ice thickness retrieval algorithms and not be used in the sense of a fully calibrated and validated data product. It is our aim however, to implement progress in algorithm development in new revisions and provide robust uncertainty estimations for CryoSat-2 freeboard and sea ice thickness.

We encourage users to give feedback (info@meereisportal.de) for further improvements of the AWI CryoSat-2 level-2 sea ice processor.

Changelog

Version 1.2 (2016-06-09)

Algorithm

- Corrected an error in the TFMRA retracker, where the filter window size (*ws=10*) for the waveform smoothing resulted in a small range bias due to an asymmetric location of the filter window (w=[i-5:i+4]). The window size in v1.2 is set to an odd number (*ws=11*) to result in a symmetric filter window (w=[i-5:i+5]). The magnitude of the filter bias depends on the steepness of the leading edge and thus is variable for different sea ice types. The effect of the correction is illustrated in section 3.2.

Auxiliary Data

- The mean sea surface product version has been changed from DTU13 to DTU15 to address issue # I-1. The effect of the new mean sea surface product is illustrated in section 3.1.

Time Series

- The CryoSat-2 time series has been updated until April 2016
- Monthly grids are only produced from October through April

Output

- Changed output data format to netCDF4 with enabled compression leading to significantly smaller files.

Version 1.1 (2015-08-15)

Algorithm

- The processing generally follows the methods described in Ricker et. al (2014)
- The penetration factor p is not used in rev1.1 (in consistence with Ricker et al. (2014)). The decision was made since the parameter is not considered to be validated enough for all regions and seasons other than spring. Instead it is assumed the main radar backscattering horizon is the snow-interface though this might lead to a bias in the freeboard data.
- The TSRA retracker algorithm is replaced by the TFMRA (Threshold-First-maximum-Retracker), using a 50 % threshold (see Ricker et al. (2014) and Helm et al. (2014))
- Smooth width of the linear interpolation of the lead elevations has been reduced from 100 km to 25 km.
- Added a correction term to the freeboard for taking into account the lower propagation speed inside the snow layer.
- Gridding is now performed using a weighted mean for each grid cell by considering the individual uncertainties.

Auxiliary Data

- The version of the mean sea surface is upgraded from DTU10 to DTU13

Output Parameter

- New fields have been added to the netcdf file, containing the fractions of the different surface types within a grid cell (see Data Description section)

Time Series

- The CryoSat-2 time series has been updated until May 2015

Known Issues

#	Issue	Description	Affected	Status
I-1	**Artefact in the DTU10/DTU13 MSS**	Due to interpolation artefacts in the DTU 13 mean sea-surface height, in particular at 86°N, steep gradients in the MSS cause artefacts in the sea-ice freeboard and thickness retrieval, in particular at 86°N.	v1.0 – v1.1	Resolved in v1.2
I-2	**Waveform retracking**	The retracking algorithm (TFMRA) has yet to be fully validated and a systematic bias in sea-ice freeboard and thickness cannot be ruled out.	v1.0 – v1.2	Open
I-3	**Snow volume scattering**	For the freeboard-to-thickness conversion, we assume that the main scattering horizon is located at the snow-ice interface. Therefore, any shift of the main scattering horizon towards the snow surface due to volume scattering can lead to systematic overestimation of sea-ice freeboard and thickness. Preliminary investigations show in fact that TFMRA ice freeboard is likely biased high, though the contribution of retracker uncertainty and snow volume fraction is ambiguous.	v1.0 – v1.2	Open
I-4	**CryoSat-2 baseline-C surface type classification**	The multi-parameter thresholds defined in Ricker et al, 2014 are based on waveforms parameters of CryoSat-2 baseline-B data. Updates in ESA's baseline-C data version lead to difference in waveform shape and thus to the surface type classification of the AWI CryoSat-2 sea ice data product. An impact analysis caused by the change in ESA algorithm baseline is pending.	v1.1 – v1.2	Open

Issues with the data content / format can be reported at info@meereisportal.de

1 Introduction

1.1 Purpose of this Document

Purpose of this document is the documentation of the CryoSat-2 level-2 processor developed at the Alfred Wegener Institute for Polar and Marine Research and data release of Arctic sea ice freeboard & thickness. This document will give a short description of the algorithm and methods applied to infer CryoSat-2 sea-ice freeboard and conversion into sea-ice thickness including the corresponding uncertainties. The results of the AWI CryoSat-2 level-2 processor processing are publically available for download and a technical description of the data format is given here.

This document is aimed to the scientific community, therefore only a brief algorithm outline is given. Interested readers, who seek a comprehensive introduction in the principle of CryoSat-2 sea ice thickness retrieval, should refer to the ESA CryoSat-2 website.

1.2 Scope of the AWI CryoSat-2 Sea-Ice Thickness Data Product

The development of a sea-ice level-2 (freeboard & thickness) processor was started at the Alfred Wegener Institute (AWI) with the goal of estimating uncertainties of CryoSat-2 data over sea ice. AWI is engaged in several validation activities of CryoSat-2 for land and sea ice in the framework of the CryoSat Validation Experiment (CryoVEx).

1.3 Further Information

For all information of the CryoSat-2 mission and ESA data products please refer to the *CryoSat Product Handbook*, which is available for download at the ESA Earthnet Online. Additional information can be found on the following websites:

German CryoSat-2 Project Office

ESA – Living Planet Programme - CryoSat

UCL - CryoSat Performance and Quality Monitoring

2 AWI Sea-Ice Level-2 Processor

The AWI sea-ice level-2 processor consists of two major steps:

1. Estimation of sea-ice freeboard from CryoSat-2 radar waveforms
2. The conversion of sea-ice freeboard into sea-ice thickness with auxiliary datasets

The first step requires the processing of all available CryoSat-2 level-1b data over Arctic sea ice, while the second step consists of the interpretation of the retrieved freeboard values. Both steps require assumptions and simplifications, which are based on results of validation activities by ESA and partner organizations. These are described in the following sections. It is a major goal of this processor to estimate not only sea-ice thickness, but also the quantification of uncertainties, which arise from of the quality of the level-1b and the necessary assumptions and simplifications.

2.1 Freeboard Retrieval

2.1.1 Getting Elevation from CryoSat-2 data

Since product version 1.2 we use ESA SAR and SARIn waveforms of the current algorithm baseline C, while v1.1 was based on baseline-B/baseline-C and v1.0 solely on baseline-B.. We apply a Threshold-First-Maximum Retracker (TFMRA, Ricker et al., 2014, Helm et al., 2014), which ties the main scattering horizon at 50 % of the first maximum peak power of the waveform, considering the noise floor. This means that the mean distance to the ice surface is assumed to be at this retracked position. The TFMRA is applied for all surface types (water, sea ice, mixed) to estimate the ellipsoidal elevation L.

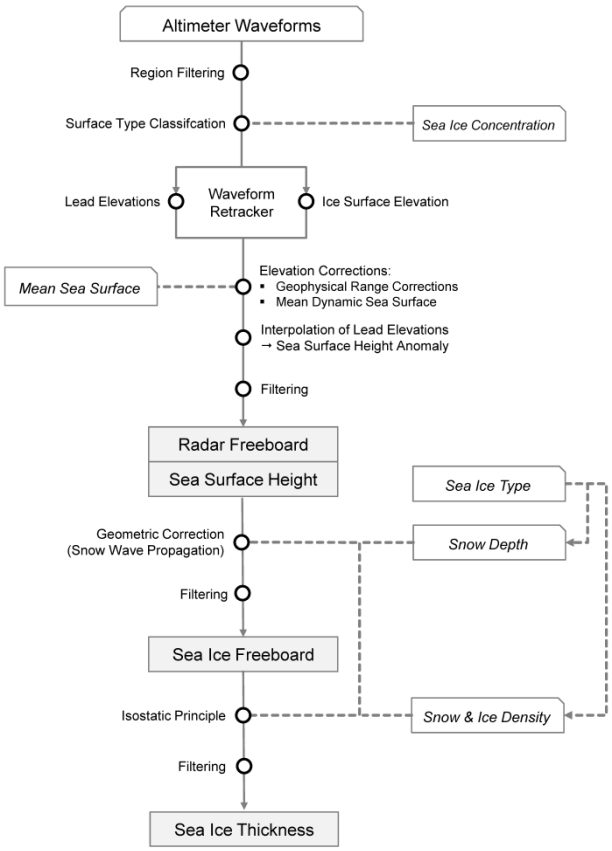

Figure 1: AWI CryoSat-2 sea ice level-2 processor scheme (Ricker et al., 2014)

2.2 From Elevation to Freeboard

In order to obtain sea-ice freeboard, the elevation L must be referenced to the local sea-surface height. This is done in two steps:

1. Subtraction of the mean sea-surface height product DTU15 (MSS) from the elevation L to remove the major undulations in the sea-surface height, mainly caused by the geoid.
2. Automatic detection of open water spots in the ice cover (leads). The elevations of leads define the sea-surface anomaly (SSA), which is the deviation of the actual sea-surface height from the mean sea-surface height.

The first step reduces errors in the detection of the leads and uncertainties in areas, where leads are scarce. Moreover, it reduces interpolation errors between discrete lead elevations (step 2). The second step accounts for deviations (SSA) of the actual local sea-surface height and is calculated for each CryoSat-2 ground track individually.

The subtraction of mean sea-surface height (MSS) and sea-surface anomaly (SSA) from the elevations L subsequently yield the height of the sea-ice surface as seen by the radar altimeter. No assumptions or corrections according to snow volume scattering are made. Therefore, we assume that the main scattering horizon is given by the snow-ice interface. In order to take into account the lower propagation speed in the snow, we add a correction value δ_c, which is estimated by (Kwok et al., 2014):

$$\delta_c = Z\left(1 - \frac{c_s}{c}\right) \approx 0.22\, Z$$

where c_s is the propagation speed in the snow layer and c the speed of light in vacuum. The sea-ice freeboard is then calculated by:

$$F = L - (MSS + SSA) + \delta_c$$

2.2.1 Lead Detection

The accurate retrieval of freeboard crucially depends on the classification of leads in the ice cover. Radar waves over these leads can be automatically classified by the specular shape of the radar waveforms, compared to more diffuse reflections over sea ice. These specular returns are more “peaky” than their ice counterparts and the AWI CryoSat-2 sea-ice processor uses statistical parameters of the waveform stack (namely pulse peakiness PP, Kurtosis K and standard deviation STD) in the level-1b data to automatically detect them. Leads are identified in the AWI sea-ice level-2 processor with the following settings:

$$PP \geq 40,\ K \geq 40 \text{ and } STD \leq 4$$

However, off-nadir reflections from leads can still dominate the echo and hence bias the range retrieval (snagging). Those echoes are detected and subsequently removed by calculating a modified PP on both sides of the power maximum of adjacent waveforms, the ’left’ (PP_l) and ’right’ (PP_r). The left peakiness should be high if the lead is in nadir position, though some minor contribution at the sides might be present ($PP_\mathrm{l} \geq 40$ and $PP_\mathrm{r} \geq 30$). Echoes from ice floes exhibit a lower peakiness at the tail of the waveform and therefore are identified by $PP_\mathrm{r} < 15$ and $K < 8$.

After classification for each CryoSat-2 profile, the elevations of the leads are interpolated and smoothed over a 25 km window.

2.2.2 Freeboard Uncertainty

Summarizing, the random uncertainty budget of the freeboard retrieval depends on

1. The quality of the level-1b radar echoes.
2. The skill of the SSA detection algorithm, that references the elevations to the actual sea-surface height.

Assuming uncorrelated and errors and thus standard error propagation, the random uncertainty of each individual freeboard measurement from CryoSat-2 can be described as:

$$\sigma_F^2 = \sigma_L^2 + \sigma_{SSA}^2$$

with σ_L the uncertainty for the range measurements (radar speckle) and σ_{SSA} the uncertainty of sea-surface anomaly. The SSA uncertainty is a function of the standard deviation of lead elevation and the distance to the next lead and reaches typical values between 5 and 50 cm (see table below).

	Parameter	**Value**	**Reference**
$\boldsymbol{\sigma_L}$	radar speckle	0.10 – 0.14 m	Wingham et al., 2006
$\boldsymbol{\sigma_{SSA}}$	local sea level	Variable (typically 0.05-0.5 m)	Function of distance to next detected lead

Note, that this only considers the random uncertainties. The retracking algorithm characteristics, physical signal penetration into snow and surface roughness can lead to a bias in the sea-ice freeboard/thickness retrieval (Hendricks et al., 2010, Willatt et al., 2010, 2011, Ricker et al., 2014).

2.3 Sea-Ice Thickness Conversion

Likewise, to the freeboard retrieval, the calculation of sea-ice thickness is done for each CryoSat-2 data point individually to allow point-wise uncertainty estimation. This elevation than can be used to calculate sea-ice thickness T, if the depth of the snow layer Z and the densities of sea water, sea ice and snow are known (ρ_W, ρ_I, ρ_Z):

$$T = F \cdot \frac{\rho_W}{\rho_W + \rho_I} + Z \cdot \frac{\rho_S}{\rho_W - \rho_I}$$

2.3.1 Snow Depth

The main challenge for sea-ice thickness retrieval with satellite altimeters is the parameterization of snow depth on sea ice, which is not measured routinely. There are promising efforts to use passive microwave to estimate snow depth with different approaches, but the current processors use snow climatology instead of remote-sensing data. Warren et al., 1999 established this climatology with results from drifting station mainly on multi-year sea ice collected over the past decades. However, since the Arctic Ocean shows a significant higher fraction of first-year sea ice, we follow the approach proposed by Kurtz et al., 2010 and multiply the climatological snow depth values over first year ice with a factor of 0.5.

Note: This approach is identical to Laxon et al., 2013. The climatology is given as a fit function for each month and only valid for the central Arctic Ocean. Significant error may occur if this fit is used also for region farther south (e.g. Baffin Bay), however this is included in the data product for the reason of completeness.

2.3.2 Snow and Sea-Ice Densities

The processor uses a fix value for the density of sea water (1024 kg/m^3), while the densities of sea ice are different for first-year and multi-year sea-ice regions (916.7 kg/m^3, 882.0 kg/m^3). The snow densities are retrieved from the Warren climatology (Warren et al., 1999).

2.3.3 Sea-Ice Thickness Uncertainty

The estimation of sea-ice thickness uncertainty follows the same principles as the estimation of freeboard uncertainty for each data point. A more detailed description and weighting of the different sources of uncertainty is given in Giles et al., 2007 and Ricker et al., 2014. The random thickness uncertainty depends on the uncertainty of freeboard and ice density mainly. The density of water varies not significantly and is neglected in the uncertainty budget. Other uncertainties are considered as systematic and can therefore bias the thickness retrieval, which is further considered in Ricker et al., 2014.

$$\sigma_T^2 = \left(\frac{\rho_W}{\rho_W - \rho_I}\right)^2 \cdot \sigma_F^2 + \left(\frac{F \cdot \rho_W + Z \cdot \rho_S}{(\rho_W - \rho_I)^2}\right)^2 \cdot \sigma_{\rho_I}^2$$

An estimation of the individual random uncertainties is given in the table below.

	Parameter	Value	Reference
σ_F	Freeboard	Variable	See estimation of freeboard uncertainty (this document)
σ_{ρ_I}	Sea-Ice density	FYI : 35.7 kg/m^3 MYI: 23 kg/m^3	Alexandrow et al., 2010

2.3.4 Data Gridding

The delivery of freeboard and thickness data for individual orbits is impractical due to the large amount of data, which the user would be required to download. Therefore, all parameter fields are gridded to an EASE 2.0 grid (see following section). We use the weighted arithmetic mean to calculate the average ice freeboard/thickness within one grid cell by using the individual freeboard/thickness uncertainties:

$$\overline{F},\overline{T} = \frac{\sum_{i=1}^{N} \frac{1}{\sigma^2_{[F_i,T_i]}} \cdot [F_i, T_i]}{\sum_{i=1}^{N} \frac{1}{\sigma^2_{[F_i,T_i]}}}$$

where N is the number of measurements within a grid cell. By averaging, the random uncertainties decrease with $\sqrt{N}$:

$$\sigma^2_{\overline{F},\overline{T}} = \frac{1}{\sum_{i=1}^{N} \frac{1}{\sigma^2_{[F_i,T_i]}}}$$

Note: Since the uncertainty of mean freeboard or mean thickness depends on the numbers of data points in one grid cell, the mean uncertainty cannot be projected or interpolated onto a different grid. Moreover, we only consider random uncertainties, while systematic uncertainties do not decrease by averaging.

2.4 Auxiliary Data Sources

Besides the actual CryoSat-2 level-1b data, which is available for registered users from ESA, the AWI sea-ice level-2 processor depends on the additional sea ice and ocean data sets. A list of the parameters and their sources is given below. The parameters are available in the AWI CryoSat-2 sea-ice product files projected on the output grid and averaged over one month.

Parameter	Provider
CryoSat-2 (SIRAL) level-1b data baseline-C	ESA (Access)
Sea-Ice Type	OSI-SAF (Link)
Sea-Ice concentration	OSI-SAF (Link)
Mean sea surface (MSS)	DTU15 Mean Sea Surface (Link)

3 Impact of Algorithm Changes

The following section briefly describes the impact of algorithm changes in freeboard and thickness in the AWI CryoSat-2 data product. This section has been added with the introduction of version 1.2 and only covers algorithm changes

3.1 Change of Mean Sea Surface from DTU13 to DTU15 (v1.2)

The impact of changes in the mean sea surface on freeboard retrieval is the highest in regions of

- steep gradients of the actual sea surface height
- low abundance of lead tie points to observe changes of sea surface height

A combination of both effects may lead to substantial freeboard and thickness errors as shown in the two figures below.

In this April 2015, the biggest differences are found in the multi-year sea ice zone of the Lincoln and Greenland Seas as well as in the fast ice zone in the Laptev Sea. Both regions are characterized by low lead fractions and thus a high reliance on the mean sea surface for sea surface height estimation.

Another obvious feature in the differences between freeboards and thickness obtained by using DTU13 and DTU15 is a ring-like structure north of 86°N. This is associated with changes in the input data of DTU15 and generally considered as an improvement (see issue #I-1).

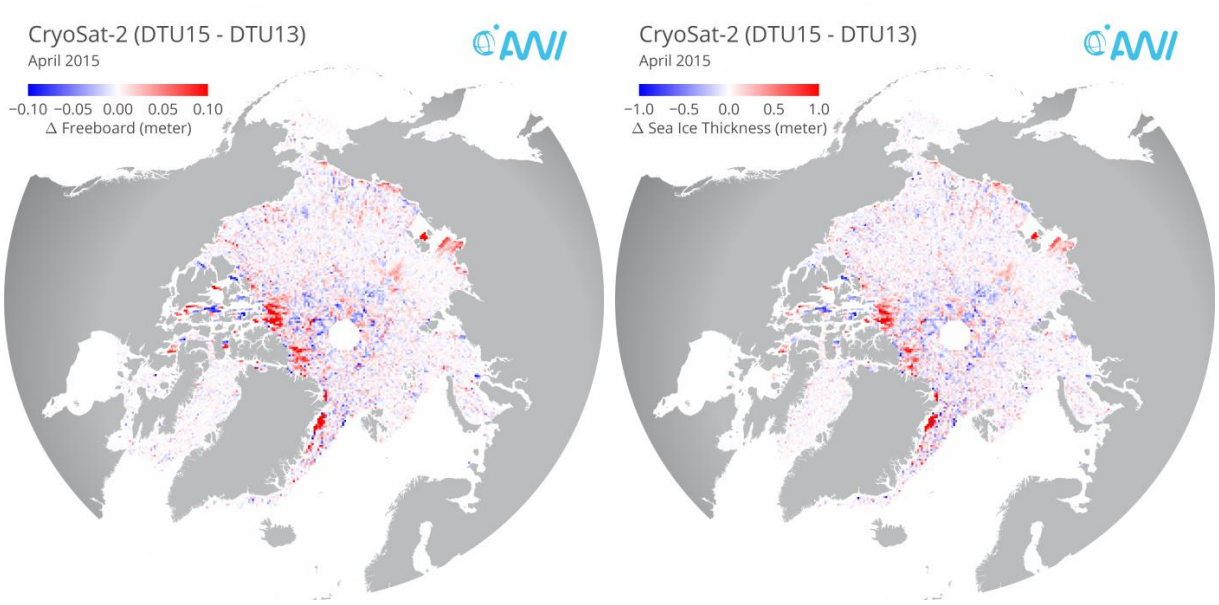

Figure 2: Impact of mean sea surface product change (DTU13 to DTU15) on freeboard and sea ice thickness

3.2 A filter window size (v1.2)

In version 1.2 the filter window size of the waveforms leading edge by the TFMRA retracker implementation was changed from an even (ws=10) to an odd (ws=11) number. Even number for block window smoother cause a slight bias since the filter window is not symmetrical around the center point and thus a small range bias is introduced. Since this range bias depends on the rate of change in power of the leading edge the bias is not constant for lead and sea ice waveforms. Thus, a fraction of this bias did propagate into freeboard and thickness fields in the data production versions 1.1 and earlier.

The bias can be significant in individual grid cells, but on average values below 1 cm for freeboard and below 10 cm for sea ice thickness are found.

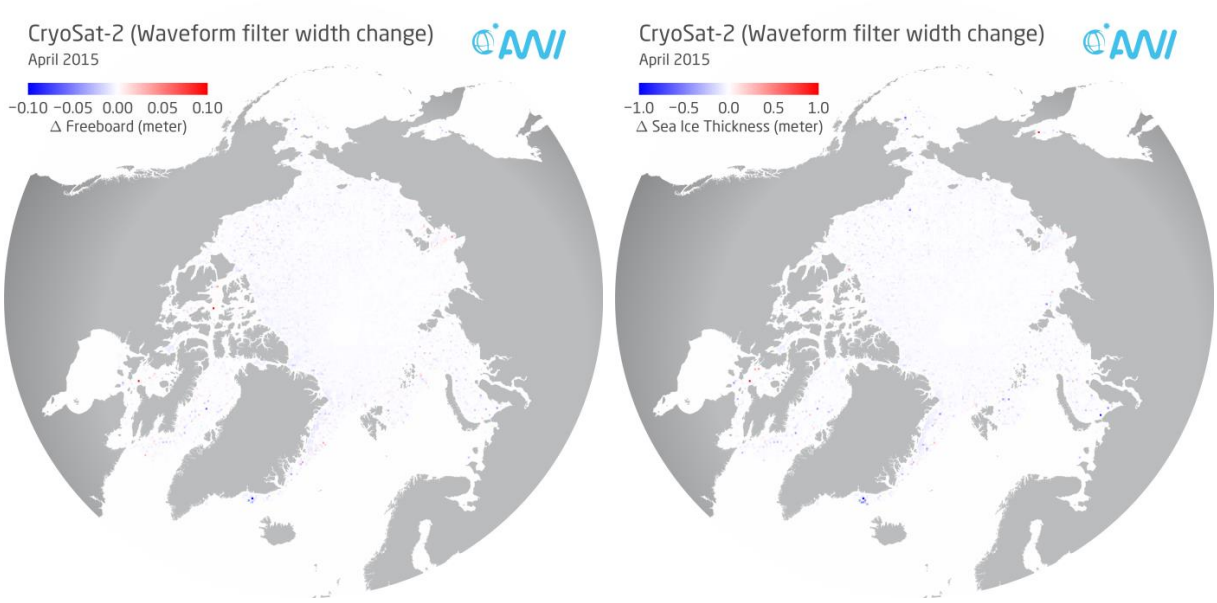

Figure 3: Impact of mean sea surface product change (DTU13 to DTU15) on freeboard and sea ice thickness

3.3 CryoSat-2 baseline-B and baseline-C data (v1.1 – v1.2)

Improvements in the L1b processing chain from baseline-B to baseline-C are summarized in ESA Document No. C2-TN-ARS-GS-5154:

https://earth.esa.int/documents/10174/1773005/C2-BaselineC_L1b_improvements_1.3

Notable changes are the introduction of surface sample stack weighting and oversampling of radar waveforms, thus affecting the retracking and the waveform-based surface-type classification. An investigation of the impact on the surface type classification result is pending, the difference in freeboard and thickness between the two input dataset versions however does not follow a regional patter, is mostly randomly distributed.

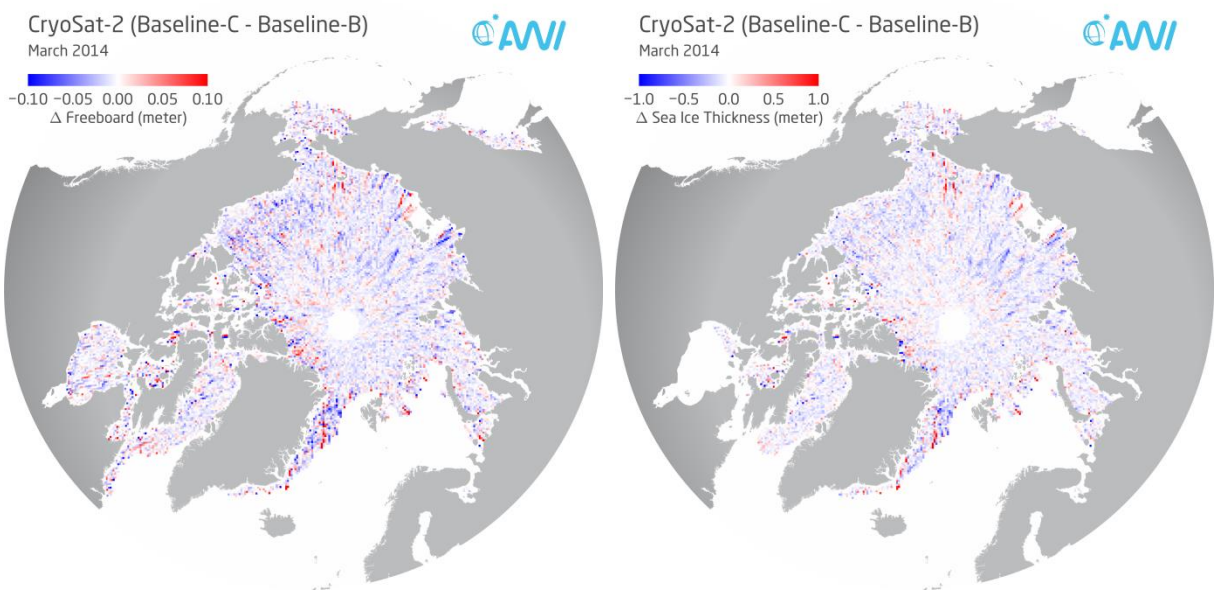

Figure 4: Impact on freeboard and sea ice thickness by CryoSat-2 L1b data product evolution from algorithm baseline-B to baseline-C

4 Data Description

4.1 Grid

For simplicity and use with other data products, all parameter fields are projected on the EASE2.0 Grid (Brodzik et al., 2012) The EASE2.0 Grid is based on a polar aspect spherical Lambert azimuthal equal-area projection and thus suitable for gridding the CryoSat-2 data on equal sized grid cells.

4.2 File Format

The data files are given a standardized binary data format (Network common data form: NetCDF v4). Specifications and software can be found at: http://www.unidata.ucar.edu/software/netcdf/. The parameters are given as grid arrays.

Parameter	Description	Unit	Type
longitude	Longitude	degrees east	Float
latitude	Latitude	degrees north	Float
sea_ice_freeboard	Sea-ice freeboard	meter	Float
fb_stat	Freeboard random uncertainty	meter	Float
fb_syst	Freeboard systematic uncertainty	meter	Float
n_valid_freeboard	Total number of valid radar freeboard data points inside one grid cell		Float
sea_ice_thickness	Sea-ice thickness	meter	Float
sit_stat	Thickness random uncertainty	meter	Float
sit_fb_syst	Thickness systematic uncertainty (freeboard)	meter	Float
n_valid_thickness	Total number of valid sea-ice thickness data points inside one grid cell		Float
sea_surface_height_anomaly	Sea-surface-height anomaly	meter	Float
sea_surface_height	Sea-surface-height	meter	Float
sea_surface_height_uncertainty	Sea-surface-height uncertainty	meter	Float
snow_depth	Snow depth (modified climatology)	meter	Float
ice_density	Ice density (modified climatology)	kg/m^3	Float
snow_density	Snow density (Warren climatology)	kg/m^3	Float
sea_ice_type	Sea-ice type		Float
sea_ice_concentration	Sea-ice-concentration	percent	Float
floe_fraction	Floe fraction inside one grid cell	fraction	Float
disc_fraction	Discarded waveforms fraction inside one grid cell	fraction	Float
lead_fraction	Lead fraction inside one grid cell	fraction	Float
ocean_fraction	Ocean fraction inside one grid cell	fraction	Float
n_valid_waveforms	Total number of all valid waveforms inside one grid cell	fraction	Float
n_waveforms	Total number of all waveforms inside one grid cell	fraction	Float
n_valid_waveforms	Total number of all valid waveforms inside one grid cell	fraction	Float

5 Parameter & Abbreviation Index

Parameter	Description
L	Surface elevation of retracked level-1b data
MSS	Mean sea surface height
SSA	Sea surface anomaly
F	Sea-ice freeboard
FYI	First-year sea ice
MYI	Multiyear sea ice
Z	Snow depth
PP	Pulse peakiness
T	Sea ice thickness
$TFMRA$	Treshold first maximum retracker algorithm
ρ_W	Density of sea water
ρ_I	Density of sea ice
ρ_S	Density of snow
σ_L	Uncertainty surface elevation
σ_F	Uncertainty freeboard
σ_{SSA}	Uncertainty sea surface anomaly
σ_Z	Uncertainty snow depth
σ_T	Uncertainty sea ice thickness
σ_{ρ}	Uncertainty sea water density
σ_{ρ_I}	Uncertainty sea ice density
σ_{ρ_S}	Uncertainty snow density

6 References

Alexandrov, V., Sandven, S., Wahlin, J., and Johannessen, O. M. (2010). The relation between sea ice thickness and freeboard in the arctic. The Cryosphere, 4:373–380.

Brodzik, M. J., Billingsley, B., Haran, T., Raup, B., and Savoie, M. H.: EASE-Grid 2.0: Incremental but Significant Improvements for Earth-Gridded Data Sets, ISPRS International Journal of Geo- Information, 1, 32–45, doi:10.3390/ijgi1010032, http://www.mdpi.com/2220-9964/1/1/32, 2012.

Giles, K.; Laxon, S.; Wingham, D.; Wallis, D.; Krabill, W.; Leuschen, C.; McAdoo, D.; Manizade, S. & Raney, R. Combined airborne laser and radar altimeter measurements over the Fram Strait in May 2002 Remote Sensing of Enviroment, 2007, 111, 182-194

Helm, V., Humbert, A., and Miller, H.: Elevation and elevation change of Greenland and Antarctica derived from CryoSat-2, The Cryosphere, 8, 1539–1559, doi: 10.5194/tc-8-1539-2014, URL http://www.the-cryosphere.net/8/1539/2014/, 2014.

Hendricks, S.; Stenseng, L.; Helm, V.; Haas, C., "Effects of surface roughness on sea ice freeboard retrieval with an Airborne Ku-Band SAR radar altimeter," *Geoscience and Remote Sensing Symposium (IGARSS), 2010 IEEE International* , vol., no., pp.3126,3129, 25-30 July 2010, doi: 10.1109/IGARSS.2010.5654350

Kurtz, N. T., and S. L. Farrell (2011), Large-scale surveys of snow depth on Arctic sea ice from Operation IceBridge, Geophys Res Lett, 38.

Kwok, R.: Simulated effects of a snow layer on retrieval of CryoSat-2 sea ice freeboard, Geophysical Research Letters, 41, 5014–5020, doi: 10.1002/2014GL060993, URL http://dx.doi.org/10.1002/2014GL060993, 2014.

Laxon S. W., K. A. Giles, A. L. Ridout, D. J. Wingham, R. Willatt, R. Cullen, R. Kwok, A. Schweiger, J. Zhang, C. Haas, S. Hendricks, R. Krishfield, N. Kurtz, S. Farrell and M. Davidson (2013), CryoSat-2 estimates of Arctic sea ice thickness and volume, Geophys. Res. Lett., 40, 732–737, doi:10.1002/grl.50193

Ricker, R., Hendricks, S., Helm, V., Skourup, H., and Davidson, M.: Sensitivity of CryoSat-2 Arctic sea-ice freeboard and thickness on radar-waveform interpretation, The Cryosphere, 8, 1607–1622, doi: 10.5194/tc-8-1607-2014, URL http://www.the-cryosphere.net/8/1607/2014/, 2014.

Warren, S.; Rigor, I.; Untersteiner, N.; Radionov, V.; Bryazgin, N.; Aleksandrov, V. & Colony, R. Snow depth on Arctic sea ice, *Journal of Climate,* 1999*, 12*, 1814-1829

Willatt, R.C.; Giles, K.A.; Laxon, S.W.; Stone-Drake, L.; Worby, A.P., "Field Investigations of Ku-Band Radar Penetration Into Snow Cover on Antarctic Sea Ice," *Geoscience and Remote Sensing, IEEE Transactions on* , vol.48, no.1, pp.365,372, Jan. 2010, doi: 10.1109/TGRS.2009.202

Willatt, R and Laxon, S and Giles, K and Cullen, R and Haas, C and Helm, V (2011) Ku-band radar penetration into snow cover Arctic sea ice using airborne data. Annals of Glaciology, 52 (57) 197 - 205., doi:10.3189/172756411795931589.

Wingham, D.; Francis, C.; Baker, S.; Bouzinac, C.; Brockley, D.; Cullen, R.; Chateau-Thierry, P. de.; Laxon, S.; Mallow, U.; Mavrocordatos, C.; Phalippou, L.; Ratier, G.; Rey, L.; Rostan, F.; Viau, P. & Wallis, D. CryoSat: A mission to determine the fluctuations in Earths's land and marine ice fields Adv. Space Res., 2006, 37, 841-871